

## The effects of Zn and Mg on the mechanical properties of the Al/TiN interface: a first-principles study

This article has been downloaded from IOPscience. Please scroll down to see the full text article.

2007 J. Phys.: Condens. Matter 19 226003

(<http://iopscience.iop.org/0953-8984/19/22/226003>)

View [the table of contents for this issue](#), or go to the [journal homepage](#) for more

Download details:

IP Address: 129.252.86.83

The article was downloaded on 28/05/2010 at 19:07

Please note that [terms and conditions apply](#).

# The effects of Zn and Mg on the mechanical properties of the Al/TiN interface: a first-principles study

H Z Zhang<sup>1</sup> and S Q Wang

Shenyang National Laboratory for Materials Science, Institute of Metal Research,  
Chinese Academy of Sciences, Shenyang 110016, People's Republic of China

E-mail: [hzzhang@imr.ac.cn](mailto:hzzhang@imr.ac.cn)

Received 21 September 2006, in final form 13 March 2007

Published 3 May 2007

Online at [stacks.iop.org/JPhysCM/19/226003](http://stacks.iop.org/JPhysCM/19/226003)

## Abstract

The adhesion and tensile behaviours of Zn and Mg contaminated Al/TiN(001) interfaces are investigated by first-principles calculations. The structures of the monolayer and half-monolayer Zn and Mg at the interface are studied. The results show that Zn and Mg greatly affect the adhesion and mechanical properties of the Al/TiN(001) interface. Both Zn and Mg increase the interfacial separation and decrease interface adhesion. During the tensile simulation, fractures of the Zn and Mg contaminated Al/TiN(001) interfaces are caused by the rupture of interface Zn–N and Mg–N bonds. The tensile strengths of them are smaller than that of the clean Al/TiN(001) interface. The Mg contaminated interfaces have higher work of adhesion and larger tensile strength than the Zn contaminated ones. The calculations are consistent with the experimental results and provide an insight from the atomic and electronic points of view.

(Some figures in this article are in colour only in the electronic version)

## 1. Introduction

Metal–ceramic interface materials, such as multi-layers, thin films and coating materials, have extraordinary mechanical, electric and optical properties. They are widely used in various fields, for instance, in electronic devices, structural materials and catalysts [1–9]. Because the characteristics of the interfaces greatly affect the properties of these materials, the metal–ceramic interfaces attract great attention from both experimental [1–5] and theoretical [6–9] aspects.

In the past ten years, density functional theory (DFT) simulations have played important roles in the field of surface and interface research [6–9]. Recently, many interface systems, such as metal/Al<sub>2</sub>O<sub>3</sub> [10–13], NiAl/Cr [14], Al/VC(N) [15], metal/TiC(N) [16], Fe/VN [17] and Cu/MgO [18], have been studied. However, heterogeneous interfaces with impurity atoms have seldom been simulated. Up to now, only a few calculations have been performed in this

<sup>1</sup> Author to whom any correspondence should be addressed.

field [19–24]. The influence of S on the adhesion of Ni/Al<sub>2</sub>O<sub>3</sub> interface has been studied [19]. It was concluded that the defects at the interface strongly influence the properties of the interface. The effects of B, C, N, O and S atoms on the Mo/MoSi<sub>2</sub>(001) [20], Fe/Al(100) [21] and Al/Al<sub>2</sub>O<sub>3</sub> interfaces [22] have been investigated. It was found that S atoms decrease the interface strength and C, O and B atoms increase interface adhesion. Further, the early transition metals (Sc, Y, Ti, and Zr) at the Ni/Al<sub>2</sub>O<sub>3</sub> interface have been investigated [23, 24]. Most previous simulations have focused mainly on the effects of impurities on the work of adhesion, but a few investigations have been performed on the variation of the tensile properties of interfaces. On the other hand, there have been a lot of DFT investigations on the tensile and shear properties of materials [25–29]. These calculations provided important information of the deformation process, ideal strength and the variation of electronic structures of materials under external stress. In fact, metal–ceramic composites often fracture during the tensile process, so it is necessary to study the effects of defects on the mechanical properties using state-of-art DFT calculations.

To improve its mechanical properties of Al/TiN, many experiments have been performed [30–35]. Because the additions of alloy elements can improve the properties of pure Al such as hardness and corrosion resistance, Al alloy are usually employed to synthesize the Al/TiN interface materials. It was reported that impurities of alloy elements at the interface affect the interfacial chemical bond and change the properties of interface materials [36–39]. Mg and Zn are important alloy components of super-hard Al alloys. The wetting ability of TiC by Al–Mg alloy was investigated using an Al–Mg alloy containing 1–20 wt% of Mg [40, 41]. It was found that Mg might segregate and form MgAl<sub>2</sub> phases at the interface. The effects of impurities on the heterogeneous interfaces have been widely investigated using computational simulation. Harter *et al* used a monolayer structure to study the effects of H on the diamond/Al interface [42, 43]. Carter *et al* used a half-monolayer structure to investigate the effects of Sc, Ti, Y, Zr, and Si on the Al<sub>2</sub>O<sub>3</sub>/Ni interface [23, 24]. Liu *et al* systematically studied the interfacial structure and Al/TiN and Al/TiC interface adhesion by first-principles calculations [44–46]. Based on these studies, we simulate the Zn and Mg contaminated Al/TiN(001) interfaces using the same model of monolayer and half-monolayer coverage of impurities at interface; such a model corresponds to a high concentration of impurity. The purpose of this study is to investigate the effects of high concentration of Mg and Zn on the adhesion and mechanical properties of the Al/TiN(001) interface.

The remainder of this paper is organized as follows. In section 2, we first describe the computational methodology used in this study. Then the interfacial structure, electronic properties and adhesion of the Zn and Mg contaminated interfaces are presented in section 3. The tensile calculations are presented in section 4. Finally, we summarize our study in section 5.

## 2. Methodology

The package Dacapo [47] is utilized in this work; it is based on DFT [48, 49], which uses a plane-wave (PW) basis set for the expansion of the single-particle Kohn–Sham wavefunctions and Vanderbilt ultrasoft pseudopotentials (US PPs) [50] to describe ionic cores. The exchange–correlation energy is described by the generalized gradient approximation of Perdew and Wang (GGA-PW91) [51]. The self-consistent PW91 density is determined by iterative diagonalization of the Kohn–Sham Hamiltonian, coupled with a Pulay mixing scheme [52]. A Fermi function is used with a temperature-broadening parameter of 0.2 eV to improve the convergence. Atomic geometries are relaxed by quasi-Newton method [53] based on Broyden–Fletcher–Goldfarb–Shanno methodology [54]. The Brillouin zone is sampled with a Monkhorst–Pack  $k$ -point grid [55]. For the bulk, a  $[8 \times 8 \times 8]$   $k$ -point mesh is used, and

a  $[8 \times 8 \times 1]$   $k$ -point mesh is used for the surface or interface. The plane-wave cutoff in our calculations is 350 eV. This set of parameters assures a total energy convergence of 0.01 eV per atom. In previous studies [45, 46], the pseudopotentials for both bulk TiN and Al were fully tested and they showed good agreements with other calculations and experiments. The same pseudopotentials are used in this study.

### 3. Interface structure and adhesion

#### 3.1. Model geometry

In previous studies, it was found that an Al atom on a N atom (N-site) is the most energy favourable structure for the Al/TiN(001) interface [44]. In this study, we investigate the interface system based on this optimal structure. Seven layers of Al(001) are placed on seven layers TiN(001), and there is no vacuum between the slabs. The monolayer and half-monolayer Zn and Mg contaminated interfaces are studied. For the monolayer impurity structure [42, 43], the impurity atom is introduced into the  $(1 \times 1)$  Al/TiN(001) interface through the substitution of Zn or Mg for the interfacial Al atom. The half-monolayer impurities structures [23, 24] are constructed by the substitution of Zn or Mg for one of the interfacial Al atoms in the  $(2 \times 1)$  Al/TiN(001) system.

#### 3.2. Work of adhesion

The ideal work of adhesion,  $W_{\text{ad}}$ , is a basic and fundamental quantity to predict adhesion of an interface. It is defined as the reversible work needed to separate an interface into two free surfaces.  $W_{\text{ad}}$  can be given by the difference in total energy between the interface and its isolated slabs [7]:

$$W_{\text{ad}} = (E_A^{\text{tot}} + E_B^{\text{tot}} - E_{A/B}^{\text{tot}})/2S. \quad (1)$$

Here,  $E_A^{\text{tot}}$  and  $E_B^{\text{tot}}$  are the total energy of the relaxed, isolated TiN and Al slabs in the same supercell when one of the slabs is kept and the other one is replaced by vacuum, respectively, and  $E_{A/B}^{\text{tot}}$  is the total energy of the interface system.  $S$  is the interface area of the unit cell. For the clean Al/TiN(001) N-site interface, the calculated  $W_{\text{ad}}$  is  $1.31 \text{ J m}^{-2}$ , which is consistent with the experimental value of  $1.51 \text{ J m}^{-2}$  [56], and the calculated interfacial separation is  $1.98 \text{ \AA}$ .

**3.2.1. Adhesion of Zn system.** For the Zn contaminated interface, when the coverage of Zn is a monolayer (ML), the calculated fully relaxed interfacial separation (Zn–N bond) is  $2.13 \text{ \AA}$ , and  $W_{\text{ad}}$  is  $0.91 \text{ J m}^{-2}$ . And when the coverage of Zn is a half-monolayer, the values are  $2.08 \text{ \AA}$  and  $1.02 \text{ J m}^{-2}$ , respectively. So the interfacial Zn atom increases the interfacial separation and decreases the interface adhesion compared with the clean Al/TiN(001) interface.

To clearly describe the chemical bonds of the interface, the local density of states (LDOS) of the interface Zn and N atoms and the sub-interface Al atom are shown in figure 1(a). For the 1.0 ML Zn contaminated interface, from  $-16$  to  $-14$  eV and  $-8$  to  $-2$  eV, there are the chemical bonds of the hybridization of Zn(4s) and N(2sp). The interface Zn and sub-interface Al share some overlapping states from  $-8$  eV to the Fermi energy, which is the metallic bond between Al and Zn.

**3.2.2. Adhesion of Mg system.** For the Mg contaminated interface, when the coverage of Mg is a monolayer, the interfacial separation (Mg–N bond) is  $2.23 \text{ \AA}$ , and  $W_{\text{ad}}$  is  $1.18 \text{ J m}^{-2}$ .

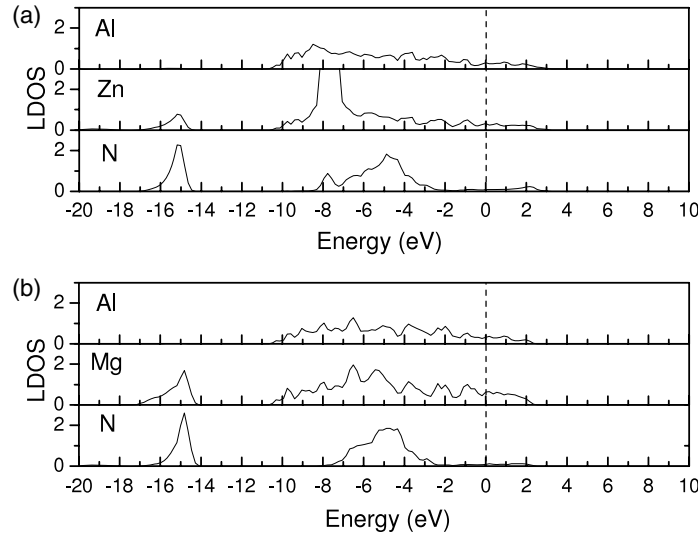


**Figure 1.** (a) LDOS of interfacial N, Zn, and the sub-interface Al atoms; (b) LDOS of interfacial N, Mg, and the sub-interface Al atoms of the 1.0 ML Zn and Mg contaminated interfaces.

When the coverage of Mg is a half-monolayer, the values are  $2.10 \text{ \AA}$  and  $1.14 \text{ J m}^{-2}$ . The results of this work are consistent with the instance of Mg segregation at the Al/TiC(001) interface [40, 57]; these studies also found that the Mg atom increases the interfacial separation and decreases  $W_{\text{ad}}$ . Experiments reported that different types of Al alloys have different wetting abilities on a TiC substrate. The wetting abilities of Al alloys on TiC are generally decreased compared with pure Al. Some of the Al alloy elements weaken the adhesion of Al on TiC substrate [36–38]. The results of this study show that both the Mg and Zn elements decrease the adhesion of the interface.

The LDOS of the interface Mg and N atoms and the sub-interface Al atoms are shown in figure 1(b). From  $-17$  to  $-14$  eV and  $-8$  to  $-2$  eV, the interface Mg and N atoms share some overlapping states, which are the hybridized bonds between Mg(3s) and N(2sp). From  $-10$  eV to the Fermi energy, there are some overlapping states between interface Mg and sub-interface Al, which are the Al–Mg metallic bond.

The difference charge densities of the Mg and Zn contaminated Al/TiN(001) interfaces are shown in figure 2. The definition of difference charge density is given by equation (2).

$$\Delta\rho = \rho_{\text{interface}} - \rho_{\text{ceramic}} - \rho_{\text{metal}}. \quad (2)$$

Here,  $\Delta\rho$  is the difference charge density.  $\rho_{\text{interface}}$ ,  $\rho_{\text{ceramic}}$  and  $\rho_{\text{metal}}$  are the total charge density of the interface system, the isolated ceramic and isolated metal slabs of the same supercell, respectively. The electronic structure shows that, at the Mg contaminated interface, there is more charge transferring to the interface area than at the Zn contaminated interface. The interfacial Mg–N bond is stronger than the Zn–N bond. This is consistent with the results that the Mg contaminated interface has larger  $W_{\text{ad}}$  than the Zn contaminated interface.

#### 4. Tensile simulation

Since Zn and Mg change  $W_{\text{ad}}$  and the chemical bonds of the Al/TiN(001) interface, the mechanical properties are correspondingly influenced. A tensile simulation is performed to

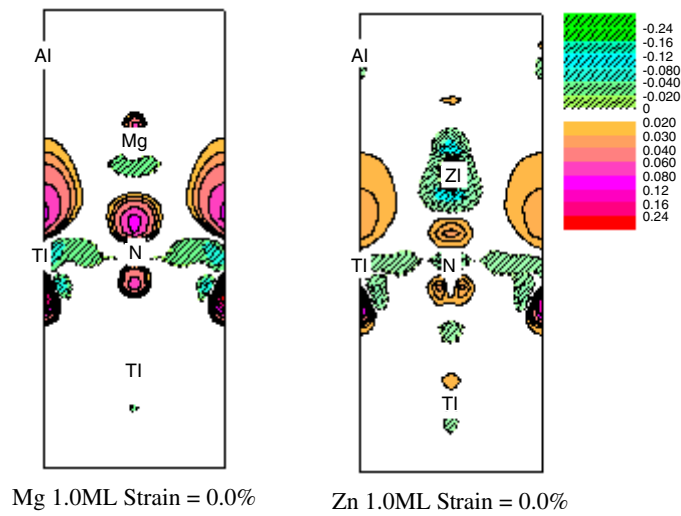


**Figure 2.** Difference charge density of the 1.0 ML Mg and Zn contaminated interfaces as defined in equation (2) at the initial stage of strain = 0.0%.

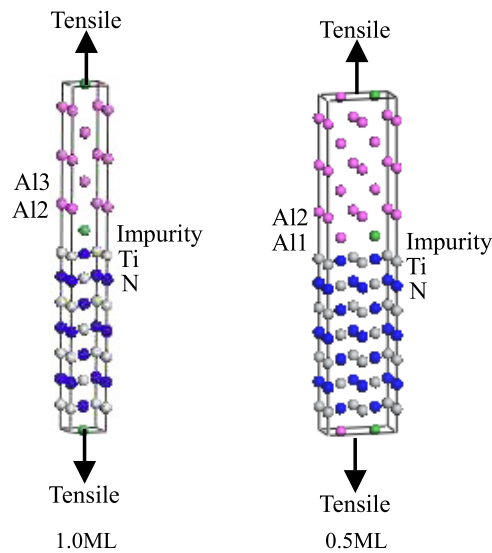


**Figure 3.** The supercell models used in the tensile test with the [001] direction of the strain. The 1.0 ML impurity contaminated (1 × 1) Al/TiN(001) interface and 0.5 ML impurity contaminated (2 × 1) Al/TiN(001) interface are shown.

investigate the tensile and fracture processes. In the tensile simulation, uniaxial strain is introduced into the supercell of the stable configuration [42, 43, 57–60]. The supercell models used in tensile test together with the direction of the strain are shown as figure 3.

First, the tensile test is simulated by gradually increasing the dimension along the  $z$ -direction. The atomic positions of the whole system are increased according to the new dimension along the  $z$ -direction, and then the atomic positions of the new configuration are

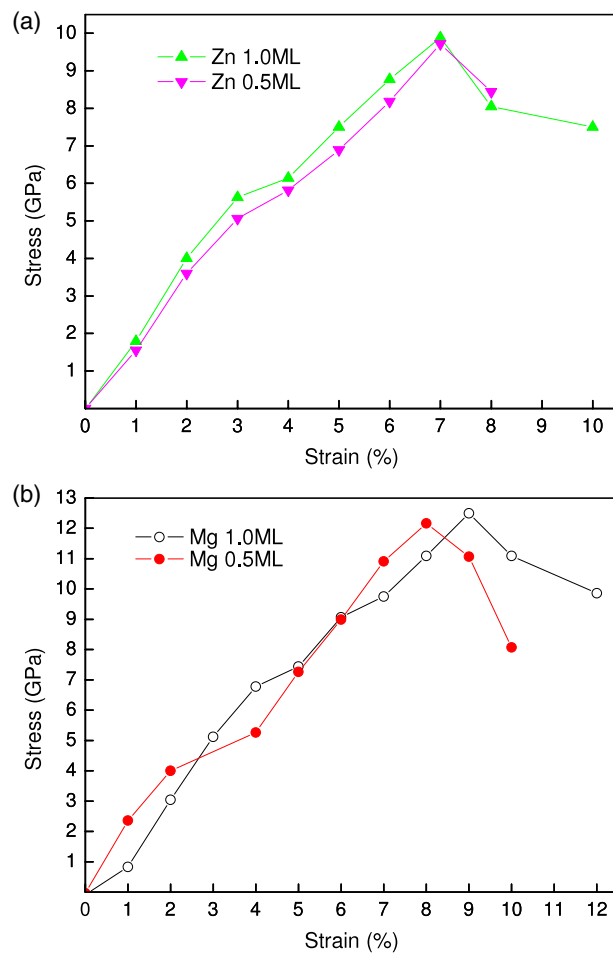


**Figure 4.** The strain–stress relationships of the 1.0 and 0.5 ML Zn and Mg contaminated Al/TiN(001) interfaces in (a) and (b), respectively.

fully relaxed at each strain stage. The next initial strain configuration will start from the former relaxed configuration. The procedure continues until the system is broken. The maximum stress is the theoretical tensile strength, which is generally higher than the experimental value. Because defects such as dislocations, vacancies and pre-cracks in the experimental samples and plastic deformation are not considered in this study, these factors can greatly decrease the tensile strength of the system. However, the theoretical tensile strength is the maximum value that the system can endure, and this value may evaluate the strength of the chemical bond.

The strain–stress relationships of the 1.0 and 0.5 ML Zn contaminated Al/TiN(001) interfaces are presented in figure 4(a), and the case of Mg contaminated system is in figure 4(b). The tensile processes of the Zn and Mg contaminated systems both experience two stages. The first stage is the deformation process, which is of an approximately linear strain–stress relationship. The fracture occurs after the stress reaches the maximum value.

The tensile strengths of the 1.0 and 0.5 ML Zn contaminated interfaces are about 9.88 and 9.72 GPa at the strain 7%, respectively. In the previous studies, the tensile strength of the clean Al/TiN(001) interfaces is about 12.56 GPa [46]. The Al terminated Cu/Al<sub>2</sub>O<sub>3</sub> interface

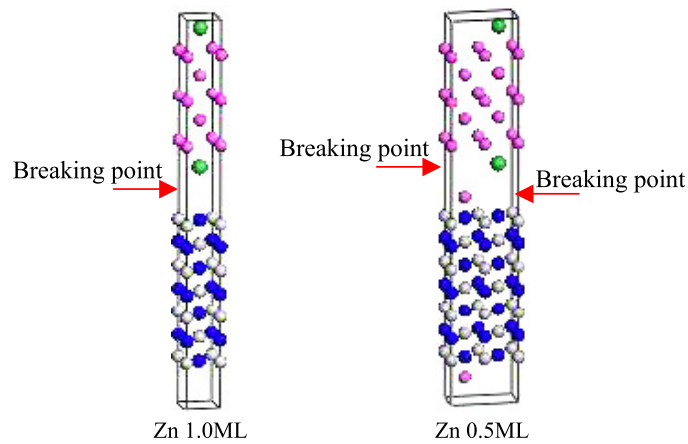


**Figure 5.** The atomic structures of the fractured 1.0 and 0.5 ML Zn contaminated Al/TiN(001) interfaces.

**Table 1.** The calculated interlayer distance (in Å) near the interface in the [001] direction at the different strain stages. The designation Al1 denotes the Al atom which is closest to the interface N atom. Al2 and Al3 are the Al atoms which are the second and third closest to the interface N atom.

| Strain (%) | Zn contaminated 0.5 ML Al/TiN(001) |       |        |         | Zn contaminated 1.0 ML Al/TiN(001) |        |         |
|------------|------------------------------------|-------|--------|---------|------------------------------------|--------|---------|
|            | Zn-N                               | Al1-N | Al2-Zn | Al1-Al2 | Zn-N                               | Al2-Zn | Al2-Al3 |
| 0.0        | 2.16                               | 2.00  | 1.82   | 1.93    | 2.03                               | 1.79   | 2.03    |
| 4.0        | 2.54                               | 2.05  | 1.81   | 2.21    | 2.28                               | 1.81   | 2.16    |
| 8.0        | 2.96                               | 2.20  | 1.90   | 2.51    | 2.60                               | 1.91   | 2.20    |
| Strain (%) | Mg contaminated 0.5 ML Al/TiN(001) |       |        |         | Mg contaminated 1.0 ML Al/TiN(001) |        |         |
|            | Mg-N                               | Al1-N | Al2-Mg | Al1-Al2 | Mg-N                               | Al2-Mg | Al2-Al3 |
| 0.0        | 2.18                               | 2.03  | 1.93   | 2.08    | 2.23                               | 2.10   | 1.98    |
| 5.0        | 2.40                               | 2.12  | 2.17   | 2.34    | 2.38                               | 2.35   | 2.10    |
| 10.0       | 2.80                               | 1.87  | 2.16   | 2.52    | 2.62                               | 2.57   | 2.15    |

has ideal tensile strength of about 10.10 GPa [60]. The Al/diamond interface has ideal tensile strength of about 12.0 GPa [42, 43]. These results are all comparable with results of this study.

To clearly show the deformation and fracture processes of the chemical bonds near the interface, the interlayer distances at the different strain stages are listed in table 1. For the Zn contaminated interface, when the coverage of Zn is 1.0 ML, the interfacial Zn-N bond is the main deformation area. Finally the fracture occurs at the mainly deformed chemical bond Zn-N. When the coverage of Zn is 0.5 ML, there are two types of interfacial chemical bond. One is Zn-N, and the other is Al1-N. It is interesting that the mainly deformed chemical bonds are Zn-N and Al1-Al2. The interface chemical bond Al1-N has a smaller deformation than the sub-interface Al1-Al2 bond. This is consistent with our previous study that the fracture of the clean Al/TiN(001) interface occurs in the sub-interface Al metal side [46]. When the deformation is large enough at strain 7%, fracture occurs at the mainly deformed chemical bond, and the breaking points are the interface Zn-N and the sub-interface Al1-Al2. The atomic structures of the fractured Zn contaminated interfaces are shown in figure 5. The tensile processes of the 0.5 ML Zn contaminated interface indicate that the fracture of the interface first occurs at the Zn-N bond, and then the breaking spreads to the Al1-Al2 bond. The 0.5 and



1.0 ML Zn contaminated interfaces have closer tensile strength which is weaker than that of the clean interface. The presence of Zn decreases the tensile strength of the Al/TiN(001) interface.

For the 1.0 and 0.5 ML Mg contaminated interface, the tensile strength is about 12.49 and 12.17 GPa at strain 9% and 8%, respectively. For the 0.5 ML Mg contaminated interface, the fracture point is at the interface Mg–N and sub-interface A11–A12 bond. For the 1.0 ML Mg contaminated interface, during the tensile stage, both the interfacial Mg–N and sub-interface A12–Mg bonds have large deformation. Finally, the fracture occurs at the interfacial Mg–N bond. The tensile strength is appreciably smaller than that of the clean interface.

## 5. Summary and conclusion

We have performed first-principles calculations of the Zn and Mg contaminated Al/TiN(001) interface. The effects of Zn and Mg on the adhesion and tensile properties of Al/TiN(001) interface are systematically investigated. Moreover, the strain–stress relationships of the impurity contaminated interfaces are established.

The results of interface adhesion show that the Zn and Mg contaminated interfaces both have smaller  $W_{ad}$  compared with that of the clean Al/TiN(001) interface. Both Zn and Mg enlarge the interfacial separation and decrease the interface adhesion. The Zn contaminated interface is weaker than the Mg system. Electronic structures also show that there is more charge distribution at the interface area of the Mg contaminated interface than that of the Zn system. Therefore, the interface Mg–N bond is stronger than the Zn–N bond. These results are consistent with the experiments that show that pure Mg/TiC interface is weaker than pure Al/TiC [39].

Further, the tensile behaviours of the Zn and Mg contaminated interfaces are investigated. The 1.0 ML Zn contaminated interfaces fractures at the Zn–N bond, and the 0.5 ML Zn contaminated one fractures at the Zn–N and A11–A12 bond. They both have smaller tensile strength than the clean interface. The 1.0 and 0.5 ML Mg contaminated interfaces have larger  $W_{ad}$  than the Zn contaminated ones. The tensile strengths of the Mg contaminated interfaces are larger than those of the Zn contaminated ones, and the breaking points are identical for both Zn and Mg contaminated interfaces. These results show that the impurities at the Al/TiN(001) interface greatly affect the adhesion and mechanical properties, which is consistent with the experimental results.

## Acknowledgments

We gratefully acknowledge the helpful and constructive discussions with Dr Limin Liu. This work is supported by the National Basic Research Program of China (No. 2006CB605103).

## References

- [1] Howe J M 1993 *Int. Mater. Rev.* **38** 233
- [2] Howe J M 1993 *Int. Mater. Rev.* **38** 257
- [3] Ernst F 1995 *Mater. Sci. Eng. R* **14** 97
- [4] Lane M 2003 *Annu. Rev. Mater. Res.* **33** 29
- [5] Ricoult M B 2003 *Annu. Rev. Mater. Res.* **33** 55
- [6] Joansson L I 1995 *Surf. Sci. Rep.* **21** 177
- [7] Finnis M W 1996 *J. Phys.: Condens. Matter* **8** 5811
- [8] Sinnott S B and Dickey E C 2003 *Mater. Sci. Eng. R* **43** 1

- [9] Lundqvist B I, Bogicevic A, Carling K, Dudiy S V, Gao S, Hartford J, Hyldgaard P, Jacobson N, Langreth D C, Lorenete N, Oversson S, Razaznejad B, Ruberto C, Rydberg H, Schroder E, Simak S I, Wahnström G and Yourdshahyan Y 2001 *Surf. Sci.* **493** 253
- [10] Feng J W, Zhang W Q and Jiang W 2005 *Phys. Rev. B* **72** 115423
- [11] Zhang W Q, Smith J R and Wang X G 2004 *Phys. Rev. B* **70** 024103
- [12] Zhang W Q and Smith J R 2000 *Phys. Rev. Lett.* **85** 3225
- [13] Zhang W, Smith J R and Evans A G 2002 *Acta Mater.* **50** 3803
- [14] Liu W, Li J C and Zheng W T 2006 *Phys. Rev. B* **73** 205421
- [15] Siegel D J, Hector L G Jr and Adams J B 2002 *Acta Mater.* **50** 619
- [16] Dudiy S V and Lundqvist B I 2004 *Phys. Rev. B* **69** 125421
- [17] Johansson Sven A E, Christensen M and Wahnström G 2005 *Phys. Rev. Lett.* **95** 226108
- [18] Benedek R, Alavi A, Seidman D N, Yang L H, Muller D A and Woodward C 2000 *Phys. Rev. Lett.* **84** 3362
- [19] Zhang W Q, Smith J R, Wang X G and Evans G A 2003 *Phys. Rev. B* **67** 245414
- [20] Hong T, Smith J R and Srolovitz D J 1993 *Phys. Rev. Lett.* **70** 615
- [21] Wang X G and Smith J R 1999 *Phys. Rev. Lett.* **82** 3105
- [22] Wang X G, Smith J R and Evans A 2002 *Phys. Rev. Lett.* **89** 286102
- [23] Jarvis E A and Carter E A 2002 *J. Phys. Chem. B* **106** 7995
- [24] Jarvis E A and Carter E A 2002 *Phys. Rev. B* **66** 100103(R)
- [25] Roundy D, Krenn C R, Cohen M L and Morris J W Jr 1999 *Phys. Rev. Lett.* **82** 2713
- [26] Kohyama M 2002 *Phys. Rev. B* **65** 184107
- [27] Ogata S, Li J and Yip S 2002 *Science* **298** 807
- [28] Ogata S, Hirotsaki N, Kover C and Shibusaki Y 2004 *Acta Mater.* **52** 233
- [29] Liao T, Wang J Y and Zhou Y C 2006 *Phys. Rev. B* **73** 214109
- [30] Oh U C and Je J H 1993 *J. Appl. Phys.* **74** 1692
- [31] Eanlisham D J, Bower J E, Marcus M A, Gross M and Merchant S 1997 *Appl. Phys. Lett.* **71** 219
- [32] Chun J S, Desjardins P, Petrov I, Greene J E, Lavoie C and Cabral C Jr 2001 *Thin Solid Films* **391** 69
- [33] Chun J S, Desjardins P, Lavoie C, Shin C S, Cabral C Jr, Petrov I and Greene J E 2001 *J. Appl. Phys.* **89** 7841
- [34] Kodambaka S, Chopp D L, Petrov I and Greene J E 2003 *Surf. Sci.* **540** L611
- [35] Avinun A, Barel N, Kaplan W D, Eizenberg M, Naik M, Guo T, Chen L Y, Mosely R, Littau K, Zhou S and Chen L 1998 *Thin Solid Films* **320** 67
- [36] Contreras A, López V H, León C A, Drew R A L and Bedolla E 2001 *Adv. Tech. Mater.* **3** 33
- [37] Leon C A, López V H, Bedolla E and Drew R A L 2002 *J. Mater. Sci.* **37** 3509
- [38] Kadolkar P and Dahotre N B 2003 *Mater. Sci. Eng. A* **342** 183
- [39] Contreras A, Leon CA, Drew RAL and Bedolla E 2003 *Scr. Mater.* **48** 1625
- [40] Contreras A, Bedolla E and Perez R 2004 *Acta Mater.* **52** 985
- [41] Contreras A, Albiter A, Bedolla E and Perez R 2004 *Adv. Eng. Mater.* **6** 767
- [42] Qi Y and Hector L G Jr 2003 *Phys. Rev. B* **68** 201403
- [43] Qi Y and Hector L G Jr 2004 *Phys. Rev. B* **69** 235401
- [44] Liu L M, Wang S Q and Ye H Q 2003 *J. Phys.: Condens. Matter* **15** 8103
- [45] Liu L M, Wang S Q and Ye H Q 2004 *Acta Mater.* **52** 3681
- [46] Zhang H Z, Liu L M and Wang S Q 2007 *Comput. Mater. Sci.* **38** 800
- [47] Hansen L *et al* 2006 *Dacapo-2.7.7* Center for Atomic Scale Materials Physics (CAMP), Demark Technical University
- [48] Hohenberg P and Kohn W 1964 *Phys. Rev.* **136** B864
- [49] Kohn W and Sham L J 1965 *Phys. Rev.* **140** A1133
- [50] Vanderbilt D 1990 *Phys. Rev. B* **41** 7892
- [51] Perdew J P, Chevary J A, Vosko S H, Jackson K A, Pederson M A, Singh D J and Fiolhais C 1992 *Phys. Rev. B* **46** 6671
- [52] Kresse G and Furthmüller J 1995 *Comput. Mater. Sci.* **6** 15
- [53] Culo P 1992 *Theor. Chim. Acta* **82** 189
- [54] Press W H, Flannery B P, Teukolsky S A and Vetterlin W T 1986 *Numerical Recipes* (Cambridge: Cambridge University Press)
- [55] Monkhorst H J and Pack J D 1976 *Phys. Rev. B* **13** 5188
- [56] Naidich Ju V 1981 *Progress in Surface and Membrane Science* (New York: Academic)
- [57] Liu L M, Wang S Q and Ye H Q 2004 *Surf. Sci.* **550** 46
- [58] Ogata S and Kitagawa H 1999 *Comput. Mater. Sci.* **15** 435
- [59] Liu L M, Wang S Q and Ye H Q 2005 *J. Phys.: Condens. Matter* **17** 5335
- [60] Yang R, Tanaka S and Kohyama M 2005 *Phil. Mag.* **85** 2961